# Temporal learning of bottom-up connections via spatially nonspecific top-down inputs

**Jung Hoon Lee**
Allen Institute for Brain Science
Seattle, WA 98019
jungl@alleninstitute.org

**Mean-Hwan Kim**
Allen Institute for Brain Science
Seattle, WA 98019
meanhwank@alleninstitute.org

**Sujith Vijayan**
School of Neuroscience, School of Biomedical Engineering and Sciences,
Department of Mathematics, and Department of Psychology
Virginia Tech
Blacksburg, VA 24060
neuron99@vt.edu

## Abstract

In the brain, high-order and low-order areas are connected via bottom-up (from low-order to high-order areas) and top-down connections (from high-order to low-order connections). While bottom-up signals are thought to be critical in generating perception, functions of top-down signals have not been clearly delineated. One popular theory is that, top-down inputs innervate a specific cell assembly to modulate responses to bottom-up inputs. However, a different line of studies proposed that not all top-down inputs are specifically delivered. As the leading theories cannot account for nonspecific top-down inputs, we seek potential functions of nonspecific top-down signals using network models in our study. Our simulation results suggest that nonspecific top-down inputs can regulate low-order area responses by providing temporal information even without spatial specificity. Specifically, the temporal information in nonspecific top-down inputs can weaken the undesired bottom-up connections, contributing to bottom-up connections' learning. We further note that cortical rhythms (synchronous oscillatory neural responses) are critical in the proposed learning process of bottom-up connections in our model.

## 1 Introduction

The brain has been thought to have hierarchical structures [6, 9, 12, 16, 29, 32], in which high-order areas rely on low-order areas for their functions. For instance, prefrontal cortex needs outputs of visual cortices to access visual information. This hierarchy of the brain has inspired deep neural networks (DNN) [23, 24], in which information propagates from input to output layers in a feedforward fashion. However, we should note that the brain is not just a group of feedforward networks. Instead, high- and low-order areas in the brain are reciprocally and intensively connected [12, 29, 28, 33], and a line of studies suggested that both bottom-up (i.e., feedforward), from low-order to high-order areas, and top-down (i.e., feedback) signals, from high-order to low-order areas, are critical in cognitive functions [4, 5, 7, 17]. Bottom-up signals have been considered responsible for sensory signal processing, but functions of top-down signals remain poorly understood.

Preprint. Under review.

A few leading theories proposed potential functions of top-down signals. First, top-down inputs can mediate selective attention or endogenous contexts, which allows sensory areas to respond selectively to more behaviorally important stimuli [14, 22]. Specifically, top-down inputs promote responses of a selected population of homogenous neurons (i.e., assembly) to win the competition among cell assemblies in low-order sensory areas; see [3] for a review. Second, top-down inputs can mediate expectations according to the predictive coding theory [8, 34]. These theories assume that top-down signals can target specific cell assemblies, but a different line of studies suggested that some top-down signals may not be target-specific [2, 1, 18, 35, 36]. Without target-specificity, they cannot mediate attention or expectation, as the earlier theories suggested, which indicates that nonspecific top-down inputs could play distinct roles. In this study, we use network models to pursue their potential functions.

Even without spatial specificity/information, top-down signals can still mediate temporal information onto target assemblies and evoke disparate responses depending on their exact arrival times. Importantly, the time-dependent efficacy of spikes can be pronounced prominently when target neurons are in synchronous and oscillatory states such as PING rhythms (oscillation at a gamma frequency generated by the interplay between excitatory and inhibitory neurons); see [37]. If top-down signals arrive, immediately after inhibitory neurons fire synchronously, they will hardly entrain target neurons due to strong inhibition. In contrast, if top-down inputs arrive, right before a rhythms' cycle, they will entrain target neurons quite reliably. Further, we note that cortical rhythms (synchronous oscillatory activities) have been thought to mediate interareal communications in the brain [13] and allow reliable learning via spike-time dependent plasticity (STDP) [26]. Inspired by this line of ideas, we hypothesize that temporal information encoded in nonspecific top-down signals can help bottom-up signals propagate effectively by modulating bottom-up connections.

To address this hypothesis, we construct a network model consisting of one low-order and one high-order area. Specifically, we consider two inhomogeneous cell assemblies in a low-order area and test the effects of nonspecific top-down signals on the evolution of connections from the two assemblies to a high-order area. Our simulation results suggest 1) that nonspecific top-down connections can suppress non-desired bottom-up connections and 2) that the difference between bottom-up connections, which reflects the degree of learning, is correlated to the power of gamma rhythms in a lower-order area. These results suggest that temporal information mediated by top-down inputs, even without spatial specificity, can make bottom-up signals more effective.

## 2 Results

To seek potential functions of nonspecific top-down inputs on bottom-up connections' learning, we use network models to study nonspecific top-down inputs' contribution to the formulation of selectivity in bottom connections. As shown in Fig. 1, our model consists of two cell assemblies in a low-order area and a single assembly in a high-order area. The two assemblies in the low-order area project to the high-order area (HA) that projects back to them via nonspecific top-down connections. Initially, the bottom-connections from both low-order area assemblies are identical and strong enough to innervate the high-order area assembly (HA), when the low-order area assemblies generate sufficiently strong outputs. With these bottom-up connections, when any of the low-order area assemblies becomes active, HA will fire. That is, the selected low-order assembly and HA will fire together, and we assume that these two connections need to be selectively strengthened, as Hebbian learning rule proposed [15]. As spike-time-dependent-plasticity (STDP) has been thought to underlie Hebbian learning in the brain [20], we implement STDP in all bottom-up connections in the model and look into nonspecific top-down inputs' contribution to bottom-up connections' learning.

In our model, we randomly choose a preferred assembly (PA) to which we introduce 500 Hz external inputs, but a non-preferred assembly (NPA) receives 100 Hz unless stated otherwise. That is, the bottom-up connections from PA to HA are expected to grow according to Hebbian learning rule. For the sake of brevity, bottom-up connections from PA and NPA will be referred to as Conn_PA and Conn_NPA, respectively, hereafter. Due to the observations that inter-area connections are layer-specific, all three assemblies consist of superficial (L2/3)

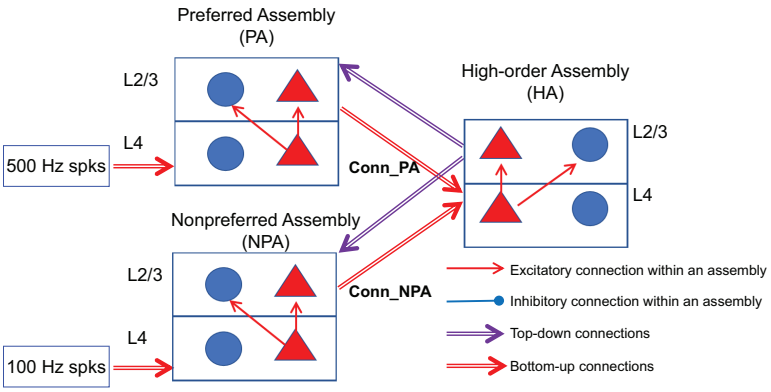


Figure 1: Schematics of the model, which consists of three assemblies (PA, NPA and HA). In superficial (L2/3) and granular (L4) layers, Pyr (red rectangles) and PV (blue circles) interact with one another. PA and NPA represent the low-order area, and they receive disparate external inputs. HA represents the high-order area. All these three assemblies interact with layer-specific top-down and bottom-up connections.

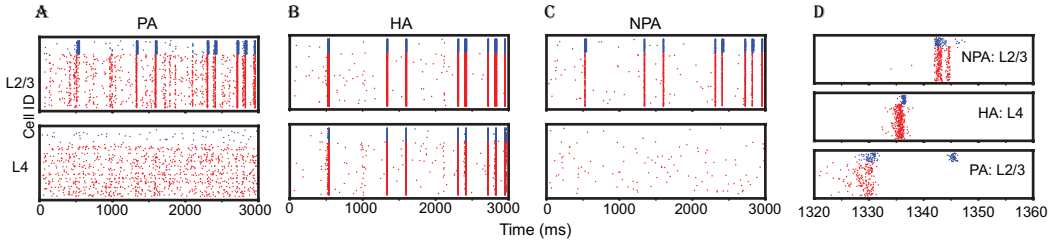


Figure 2: Raster plots of an example simulation. (A), (B), (C), spikes generated in L2/3 and L4 of PA, HA and NPA, respectively. Each dot represents a spike, and spikes from Pyr and PV neurons are shown in red and blue, respectively. For the clarity, we show them only for the first 3 seconds. (D), spikes from L2/3 of NPA and PA and those from L4 of HA, between 1320 and 1360 ms.

and granular (L4) layers, in which excitatory and inhibitory neurons interact with one another via randomly established connections (Table 1). We refer to excitatory neurons as 'Pyr' neurons, as most excitatory neurons are shaped like pyramids, and inhibitory neurons as 'PV' neurons, as most common molecular markers of inhibitory neurons are parvalbumin (PV).

We simulate the network for 20 seconds (s) to estimate how Conn_NPA and Conn_PA evolve over time with and without nonspecific top-down inputs onto both NPA and PA (Fig. 1). Fig. 2 A, B and C show the spikes from PA, HA and NPA for the first 3 s; Pyr and PV neurons are shown in red and blue, respectively. As shown in the figures, Pyr and PV neurons within each assembly fires synchronously several times. We note that the synchronous activity appears first in PA, which receives 500 Hz afferent inputs, and it subsequently appears in L4 neurons of HA and L2/3 neurons of NPA (Fig. 2D). This pattern can be readily explained by the patterns of bottom-up and top-down connections in the model. More importantly, when such sequential activations occur, according to STDP rule, Conn_PA grows stronger, whereas Conn_NPA grows weaker. Indeed, this sequential activation occurs throughout the simulation. Consequently, Conn_PA grow stronger gradually, but Conn_NPA grow weaker gradually (Fig. 3A), suggesting that bottom-up connections can be selectively strengthened with nonspecific top-down inputs.

To further examine the functions of nonspecific top-down inputs, we repeat the simulation without top-down inputs (both to PA and NPA). When top-down connections are removed from the model, Conn_PA increase as before, but Conn_NPA remain unchanged (Fig. 3B). These results suggest that nonspecific top-down connections can reduce the strengths of

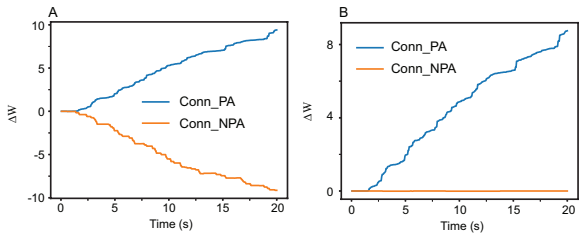


Figure 3: Time courses of bottom-up connections. (A), the mean values of bottom-up connections as a function of time. The blue and orange lines represent the mean values of bottom-up connections from PA to HA and those from NPA to HA, respectively. The mean values are calculated every 5 ms during simulations. (B), the same as (A) but without top-down connections.

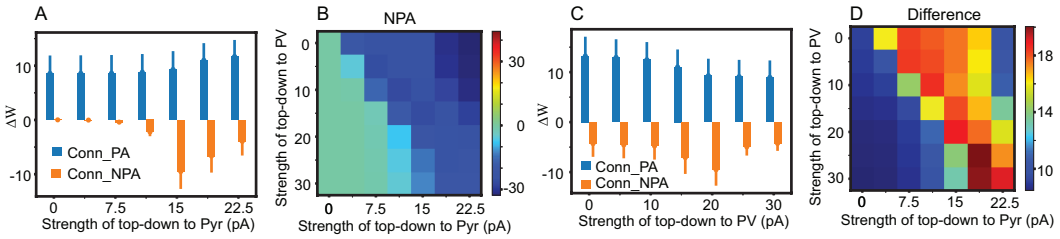


Figure 4: Dependency of bottom-up connections on strengths of top-down connections. (A), The total changes of connection strengths during simulations depending on the top-down inputs to Pyr neurons; the connection strengths are shown in pA. Blue and orange bars represent the connections from PA and NPA. The mean value and standard deviations are calculated from 20 independent simulations (Method). (B), The total changes of bottom-connections from NPA depending on to top-down connections to both Pyr and PV neurons. (C), The total changes of connection strengths during simulations depending on the top-down inputs to PV neurons (D), The difference in connection strengths between PA and NPA depending on to top-down connections to both Pyr and PV neurons.

undesired bottom-up connections (i.e., connections from NPA to HA in this model), keeping the total strength of bottom-up connections roughly the same level. We further test the effects of top-down inputs on bottom-up connections by varying the strengths of top-down connections to Pyr and PV in L2/3 of PA and NPA. To reduce statistical biases, we conduct 20 simulations, in which a network is independently constructed using the same connectivity rule (Methods). Fig. 4 shows the total changes in bottom-up connection strengths induced during 20-second-long simulations depending on the strengths of top-down connections to PV and Pyr, respectively; the mean and standard deviations from 20 independent simulations (Methods) are displayed in the figure.

We make two observations. First, without top-down inputs to Pyr neurons, the reduction of Conn_NPA is not pronounced (Fig. 4A), confirming that the delayed Pyr neurons' activity in NPA makes Conn_NPA weaker. Second, top-down inputs to PV neurons also have impact on bottom-up connections' learning (both Conn_PA and Conn_NPA). As shown in Fig. 4B, the effect of top-down inputs to PV neurons on Conn_NPA is not monotonic. Until connections reach a certain threshold ( 20 pA), the reduction of Conn_NPA's strength becomes stronger. After the threshold, the reduction becomes weaker. In contrast, as the top-down inputs to PV neurons grow, the increase in Conn_PA's strength monotonically becomes weaker (Fig. 4C). We also note that the difference between Conn_PA and Conn_NPA after 20-second-long simulations is maximal when PV and Pyr neurons receive almost the equivalent amount of top-down inputs (Fig. 4D).

The simulation results above suggest an essential role of synchronous activity in bottom-up connections' learning. Because the degree of synchronous activity is commonly measured via spectral power of local field potentials (LFPs), we simulate LFPs (Methods) and calculate

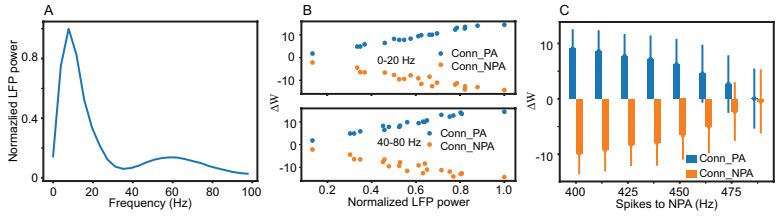


Figure 5: Contribution of synchronous oscillatory activity in learning and the robustness of learning process. (A), Spectral power of LPFs in PA normalized to the maximum value. (B), Correlations between total change of connection strengths and spectral power of LPFs in PA in two frequency bands (0-20 and 40-80 Hz). For each simulation (out of 20), we estimated the spectral power and total changes of bottom-up connection strengths. Spectral power in each frequency band is normalized to the maximum power obtained during 20 simulations. Blue and orange dots represent connections originating from PA and NPA, respectively. (C), Total changes of connection strengths depending on the external inputs to NPA; the default inputs to PA and NPA are 500 and 100 Hz.

their spectral power. As shown in Fig. 5A, PA generates oscillatory activity at two frequency bands, one at 0-20 Hz and another at 40-80 Hz. To assess how much synchronous oscillatory activity contributes to bottom-up connections' learning, we estimate the changes in strengths of bottom-up connections (Conn_PA and Conn_NPA) and the total power of two frequency bands (0-20 and 40-80 Hz) for all 20 simulations. Fig. 5B shows that the magnitudes of changes (both increase and decrease) in bottom-up connections are positively correlated with the oscillatory power in PA, supporting that cortical rhythms (i.e., synchronous oscillatory neural activity) drive bottom-up connections' learning.

In the model, if NPA, instead of PA, generates synchronous outputs, Conn_NPA, instead of Conn_PA, will become stronger. If the inputs to NPA are not strong enough, the growth of undesired connections (from NPA to HA) would be negligible on average. Then, how sensitive is this learning mechanism to the inputs to NPA? To answer this question, we increase external inputs to NPA up to 475 Hz. Fig. 5C shows that the growth of Conn_PA decreases, as the inputs to NPA grow stronger. But importantly, despite the reduction of magnitudes, the Conn_PA grow stronger, whereas Conn_NPA grow weaker, on average, even when the external inputs to NPA are 90% of those to PA. This result suggests that nonspecific top-down connections can be useful to selectively strengthen the connections even when all low-order assemblies receive relatively similar afferent inputs.

So far, we assume that only bottom-up connections have plasticity, but top-down connections can also have plasticity. That is, top-down connections can evolve over time. Naturally, two questions rise. First, will bottom-up connections change the same way? Second, how do top-down connections change? To answer these questions, we make top-down connections to have STDP and repeat the same experiments. In simulations, we impose the maximum strength of top-down connections to be 30 pA; without such limitation, the system can show run-away excitation due to strong positive feedback loops established between PA (NPA) and HA. We note 1) that bottom-up connections change as they do with stationary top-down connections (Fig. 6A and B) and 2) that top-down connections change depending on their targets (Fig. 6C and D). Specifically, top-down connections targeting NPA grow stronger, while top-down connections targeting PA grow weaker, which is consistent with an earlier experimental study [30].

## 3 Discussion

The brain is a group of recurrent networks, in which high and low order areas interact reciprocally with one another. It is generally accepted that bottom-up processing is central to generating perception as demonstrated in deep learning [23]. However, the functions of top-down inputs remain poorly understood. As most theories assume top-down inputs to be target specific, they cannot explain the functions of nonspecific top-down inputs experimentally reported [1, 2, 18, 35, 36]. Here, we employ network models to investigate

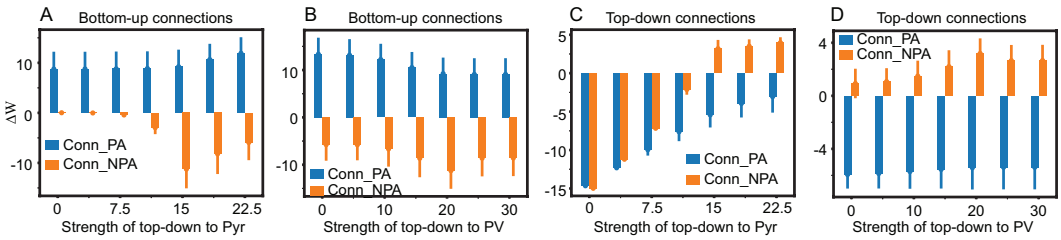


Figure 6: Simulation results with dynamically evolving top-down connections. (A), Changes of bottom connection strengths induced during long simulations, depending on initial strengths of top-down connection strengths to Pyr. Blue and orange color represent bottom-up connections originating from PA and NPA, respectively. (B), the same as (A), but depending on initial strengths of top-down connections to PV. (C), Changes of top-down connection strengths induced during simulations, depending on initial strengths of top-down connection strengths to Pyr. Blue and orange color represent top-down connections targeting PA and NPA, respectively. (D), the same as (C), but depending on initial strengths of top-down connections to PV.

how nonspecific top-down connections contribute to the dynamic organization of bottom-up connections. Our simulation results propose that nonspecific top-down inputs can mediate temporal information to low-order areas to induce the specificity in bottom-up connections. We also note that in our model STDP and cortical rhythms are essential in this learning process.

### 3.1 Functions of top-down inputs to PV neurons

In the model, nonspecific top-down inputs to Pyr neurons can reduce undesired bottom-up connections from NPA by inducing delayed activity in NPA. Additionally, the results in Fig. 4 suggest that top-down inputs to PV neurons also contribute to bottom-up connections' learning. Then, how do PV neurons contribute to this learning process? We propose that PV neurons prevent Pyr neurons' erroneous firing, which disrupts the temporal order of spikes across assemblies. If L2/3 Pyr neurons in PA fire constantly after projecting onto HA, they can fire even after HA neurons' firing. That is, the continuous firing of PA Pyr neurons can decrease Conn_PA rather than increase it. Similarly, if L2/3 Pyr neurons of NPA keep firing after HA neurons' synchronous firing, they can accidentally fire right before L4 Pyr neurons of NPA fire, leading to the increase in Conn_NPA's strength. We note that PV neurons in PA and NPA respond differently (Fig, 2D). First, in PA, PV neurons (not Pyr neurons) respond to top-down inputs. Since PV neurons in PA fire in response to top-down inputs, Pyr neurons will receive inhibition and cannot fire in response to top-down inputs. This can minimize the chance of the reduction of Conn_PA. Second, in NPA, PV neurons respond mostly to local inputs from NPA, not top-down inputs. This suggests that the active period of Pyr neurons in NPA would be short. Interestingly, the erroneous firings of Pyr neurons would occur more frequently when top-down inputs are strong. Consequently, top-down inputs to PV should be proportionally increased to ensure the proper learning of bottom-up connections, which is consistent with balanced top-down inputs to Pyr and PV neurons experimentally observed [38].

### 3.2 The function of synchronous activity in interareal connections

The communication-through-coherence (CTC) theory proposes that cortical rhythms (synchronous and oscillatory neural activity) subserve interareal interactions by increasing the efficacy of afferent inputs to target areas [13]. Consistent with this theory, synchronous activity in our model reliably propagates across assemblies via stochastic connections. More importantly, we note that synchronous activity in our model, not only enhances the efficacy of interareal communications, but also contributes to interareal connections' learning in two ways. First, when synchronous activity is generated and propagates among areas, postsynaptic neurons in the target area fire reliably after presynaptic neurons fire. This ensures the temporal gaps between pre- and postsynaptic neurons, allowing the synaptic weights

Table 1: Connections in the network model. Below, the connection probability and strength of each connection type are shown in the parenthesis. TD, BU and LGN represent top-down, bottom-up and LGN connections, respectively. Additionally, Pyr and PB neurons receive 1050 Hz and 1000 Hz background inputs, respectively, via 100 pA connections.

| | Postsynaptic Neurons | | | | |
|---|---|---|---|---|---|
| | | L2/3 Pyr | L2/3 PV | L4 Pyr | L4 PV |
| Presynaptic Neurons | L2/3 Pyr | (0.4, 40 pA) | (0.6, 40 pA) | N/A | N/A |
| | L2/3 PV | (1.0, -40 pA) | (1.0,-40 pA) | N/A | N/A |
| | L4 Pyr | (0.6, 80 pA) | (0.4, 40 pA) | (0.4, 40 pA) | (0.6, 40 pA) |
| | L4 PV | N/A | N/A | (1.0, -40 pA) | (1.0, -40 pA) |
| Across assemblies and external inputs | | | | | |
| TD to Pyr | (0.3, 15 pA) | | BU to PV | (0.3, 20 pA) | |
| TD to PV | (0.3, 20 pA) | | LGN to Pyr | (0.3, 60 pA) | |
| BU to Pyr | (0.3, 40 pA) | | LGN to PV | (0.3, 30 pA) | |

connecting them to change robustly. Second, the induced inhibition during synchronous firing prevents Pyr from erroneously firing, which makes the learning process more robust to erroneous afferent inputs. Thus, our simulation results propose a possible extension of CTC theory [13].

### 3.3 A potential coordination between specific and nonspecific top-down inputs

We find that two conditions need to be satisfied for reliable learning of bottom-up connections. First, a selected assembly should be active (or activated) more than other assemblies. Second, the most active cell assembly needs to generate synchronous activity. Conversely, the proposed learning process will not be effective when multiple assemblies receive almost the equivalent amount of afferent inputs or when the desired assembly (i.e., PA in the model) does not generate synchronous activity. However, these limits may not be so fundamental and can be dynamically regulated by selective attention, which is known to be capable of biasing competition and amplifying synchronous activity. If selective attention is directed to NPA, the synchronous activity of NPA would be amplified, and Conn_NPA, rather than Conn_PA, can become stronger. In contrast, the growth of Conn_PA can accelerate if selective attention is directed to PA. Interestingly, earlier studies proposed that top-down inputs impinging onto deep layers are target-specific [10, 21]. That is, selective attention may regulate this learning process via stimulation of deep layers. In the future, we plan to address this possibility by extending our model to incorporate deep layers and inhibitory neuron types known to be associated with interlayer interactions.

## 4 Methods

Our network model consists of three cell assemblies (Fig. 1). The two assemblies (PA, NPA) represent a low-order area, and the other (HA) represents a high-order area. PA and NPA are different only in terms of external inputs mimicking sensory inputs (Fig. 1). Based on the observations[12, 28] that bottom-up connections mainly target granular layer (L4) and that top-down connections avoid L4, we construct each assembly with two layers, superficial layer (L2/3) and L4. In each layer, excitatory neurons interact with inhibitory neurons. Commonly, excitatory neurons are referred to as pyramidal neurons due to their shape, and most inhibitory neurons are known to express parvalbumin (PV). Thus, excitatory and inhibitory neurons are referred to as Pyr and PV neurons in this study.

Each neuron type is connected to other neuron types in the same assembly. The connections are randomly established using connection probabilities determined by pre- and postsynaptic neuron types. The strengths of connections also depend on pre- and postsynaptic neuron types. The selected values for connection probabilities and strengths are listed in Table 1. The three assemblies in the model are connected with one another via inter-assembly (i.e., interareal) connections (Table 1).

Table 2: Parameters for neurons and synaptic inputs. Synaptic inputs decay ($\tau_s$) at time scales depending on presynaptic and postsynaptic neurons.

| Param | Value | Param | Value |
|---|---|---|---|
| Membrane constant | 10 ms | $\tau_s\,(Pyr \rightarrow PV)$ | 2 ms |
| Spike threshold | -50 mV | $\tau_s\,(PV \rightarrow Pyr)$ | 6 ms |
| Reset potential | -65 mV | $\tau_s\,(PV \rightarrow PV)$ | 4.3 ms |
| Refractory Period | 2 ms | Pyr cell # | 320 |
| $\tau_s\,(Pyr \rightarrow Pyr)$ | 2 ms | PV cell # | 80 |

In the model, all neurons are current-based leaky-integrate fire (LIF) neurons. The dynamics of subthreshold membrane potentials can be described by Eq. 1.

$$\frac{dV}{dt} = -\frac{V}{\tau} + \frac{I}{C}, \text{where } I = \sum_i w_+ \exp\left(-\frac{t}{\tau_{syn+}}\right) + w_- \exp\left(-\frac{t}{\tau_{syn-}}\right) \tag{1}$$

,where $w_+$ and $\tau_{syn+}$ represent the synaptic strengths and synaptic time scale of excitatory synapses; where $w_-$ and $\tau_{syn-}$ represent the synaptic strengths and synaptic time scale of inhibitory synapses. The parameters used in this study are listed in Table 2.

Excitatory (Inhibitory) synaptic events evoke instantaneous jumps (dips) of membrane potentials V and their decay over time. The inhibition and excitation decay over different time scales adopted from an earlier work [25]. The strengths of synaptic connections within assemblies are static over time, whereas the strengths of connections across assemblies are either static or dynamic depending on simulation conditions. When synaptic connections can be dynamic, the connections' strengths follow the spike-time dependent plasticity (STDP) rule summarized in Eq. 2.

$$\Delta w = \begin{cases} -\lambda f_- \times K(\Delta t) & \text{if } \Delta t \leq 0; \text{ where } K(\Delta t) = \exp(\frac{-|t|}{\tau}) \ , \\ \lambda f_+ \times K(\Delta t) & \text{if } \Delta t \geq 0, \end{cases} \tag{2}$$

, where $\Delta t = t_{post} - t_{pre}$; where $f_+(w) = (1-w)\mu, f_-(w) = \alpha\mu$. In this study, we use default values included in the NEST package ($\alpha = 1, \tau = 20.0ms, \mu = 1.0, \lambda = 0.01$).

We use peer-reviewed open-source simulation platform NEST [27] to build the network models. All parameters not specified here are taken from default parameters of NEST package [27].

Simulation of local field potentials Local field potentials (LFPs) reflect population responses. While their origins remain poorly understood, the synaptic inputs have been thought to be crucial. Consequently, we simulate LFPs by summing up all (excitatory and inhibitory) synaptic inputs to Pyr neurons included in the assemblies [11, 31]. The spectral power is calculated by the 'signal.welch' routine included in the scipy package [19].

## References


[1] Alessandra Angelucci and Paul C. Bressloff. Chapter 5 Contribution of feedforward, lateral and feedback connections to the classical receptive field center and extra-classical receptive field surround of primate V1 neurons. *Progress in Brain Research*, 154(SUPPL. A):93–120, 2006.

[2] Alessandra Angelucci and Jean Bullier. Reaching beyond the classical receptive field of V1 neurons: Horizontal or feedback axons? *Journal of Physiology Paris*, 97(2-3):141–154, 2003.

[3] Diane M. Beck and Sabine Kastner. Top-down and bottom-up mechanisms in biasing competition in the human brain. *Vision Research*, 49(10):1154–1165, 2009.

[4] Steven L. Bressler and Vinod Menon. Large-scale brain networks in cognition: emerging methods and principles. *Trends in Cognitive Sciences*, 14(6):277–290, 2010.

[5] Elizabeth a Buffalo, Pascal Fries, Rogier Landman, Hualou Liang, and Robert Desimone. A backward progression of attentional effects in the ventral stream. *Proceedings of the National Academy of Sciences of the United States of America*, 107(1):361–5, jan 2010.

[6] Ed Bullmore and Olaf Sporns. Complex brain networks: graph theoretical analysis of structural and functional systems. *Nature reviews. Neuroscience*, 10(3):186–98, 2009.

[7] Timothy J Buschman and Earl K Miller. Top-down versus bottom-up control of attention in the prefrontal and posterior parietal cortices. *Science (New York, N.Y.)*, 315(5820):1860–2, mar 2007.

[8] Andy Clark. Whatever next? Predictive brains, situated agents, and the future of cognitive science. *Behavioral and Brain Sciences*, 36(3):181–204, 2013.

[9] Gustavo Deco and Morten L. Kringelbach. Hierarchy of Information Processing in the Brain: A Novel 'Intrinsic Ignition' Framework. *Neuron*, 94(5):961–968, 2017.

[10] Laura A. Denardo, Dominic S. Berns, Katherine Deloach, and Liqun Luo. Connectivity of mouse somatosensory and prefrontal cortex examined with trans-synaptic tracing. *Nature Neuroscience*, 18(11):1687–1697, 2015.

[11] A Destexhe and C Bedard. Local field potential. *Scholarpedia*, 8(8):10183, 2013.

[12] D J Felleman and D C Van Essen. Distributed hierarchical processing in the primate cerebral cortex. *Cerebral cortex (New York, N.Y. : 1991)*, 1(1):1–47, 1991.

[13] Pascal Fries. A mechanism for cognitive dynamics: neuronal communication through neuronal coherence. *Trends in cognitive sciences*, 9(10):474–80, oct 2005.

[14] Jonathan Bridgman Fritz, Stephen V David, Jonathan B Fritz, Mounya Elhilali, Stephen V David, and Shihab A Shamma. Auditory attention – Focusing the searchlight on sound Auditory attention — focusing the searchlight on sound. *Current Opinion in Neurobiology*, (17):1–19, 2007.

[15] Wulfram Gerstner. Hebbian Learning and Plasticity. In Michael Arbib and Jimmy Bonaiuto, editors, *From neuron to cognition via computational neuroscience*, chapter 6. MIT Press, 2016.

[16] Claus-c Hilgetagl, Gully A P C Burns, Marc A O Neill, Jack W Scannell, and Malcolm P Young. Anatomical connectivity defines the organization of clusters of cortical areas in the macaque monkey and the cat. *Phil. Trans. R. Soc. Land. B*, (355):91–110, 2000.

[17] Laurence T Hunt and Benjamin Y Hayden. A distributed, hierarchical and recurrent framework for reward-based choice. *Nature reviews. Neuroscience*, 18(3):172–182, 2017.

[18] J. M. Hupé, A. C. James, B. R. Payne, S. G. Lomber, P. Girard, and J. Bullier. Cortical feedback improves discrimination between figure and background by V1, V2 and V3 neurons. *Nature*, 394(6695):784–787, 1998.

[19] Eric Jones, Travis Oliphant, Pearu Peterson, and Others. SciPy: Open source scientific tools for Python, 2001.

[20] Richard Kempter, Wulfram Gerstner, and J. van Hemmen. Hebbian learning and spiking neurons. *Physical Review E*, 59(4):4498–4514, apr 1999.

[21] Euiseok J. Kim, Ashley L. Juavinett, Espoir M. Kyubwa, Matthew W. Jacobs, and Edward M. Callaway. Three Types of Cortical Layer 5 Neurons That Differ in Brain-wide Connectivity and Function. *Neuron*, 88(6):1253–1267, 2015.

[22] Eric I. Knudsen. Fundamental Components of Attention. *Annual Review of Neuroscience*, 30(1):57–78, 2007.

[23] Yann Lecun, Yoshua Bengio, and Geoffrey Hinton. Deep learning. *Nature*, 521(7553):436–444, 2015.

[24] Yann LeCun, Leon Bottou, Yoshua Bengio, and Patric Haffner. Gradient-Based Learning Applied to Document Recognition. *PROC. OF IEEE*, 1998.

[25] Jung Hoon Lee, Christof Koch, and Stefan Mihalas. A Computational Analysis of the Function of Three Inhibitory Cell Types in Contextual Visual Processing. *Frontiers in Computational Neuroscience*, 11(28), 2017.

[26] Shane Lee, Kamal Sen, and Nancy Kopell. Cortical gamma rhythms modulate NMDAR-mediated spike timing dependent plasticity in a biophysical model. *PLoS Computational Biology*, 5(12), 2009.

[27] Charl Linssen, Mikkel Elle Lepperød, Jessica Mitchell, Jari Pronold, Jochen Martin Eppler, Chrisitan Keup, Alexander Peyser, Susanne Kunkel, Philipp Weidel, Yannick Nodem, Dennis Terhorst, Rajalekshmi Deepu, Moritz Deger, Jan Hahne, Ankur Sinha, Alberto Antonietti, Maximilian Schmidt, Luciano Paz, Jesús Garrido, Tammo Ippen, Luis Riquelme, Alex Serenko, Tobias Kühn, Itaru Kitayama, Håkon Mørk, Sebastian Spreizer, Jakob Jordan, Jeyashree Krishnan, Mario Senden, Espen Hagen, Alexey Shusharin, Stine Brekke Vennemo, Dimitri Rodarie, Abigail Morrison, Steffen Graber, Jannis Schuecker, Sandra Diaz, Barna Zajzon, and Hans Ekkehard Plesser. NEST 2.16.0. aug 2018.

[28] N. T. Markov, M. M. Ercsey-Ravasz, A. R. Ribeiro Gomes, C. Lamy, L. Magrou, J. Vezoli, P. Misery, A. Falchier, R. Quilodran, M. A. Gariel, J. Sallet, R. Gamanut, C. Huissoud, S. Clavagnier, P. Giroud, D. Sappey-Marinier, P. Barone, C. Dehay, Z. Toroczkai, K. Knoblauch, D. C. Van Essen, and H. Kennedy. A weighted and directed interareal connectivity matrix for macaque cerebral cortex. *Cerebral Cortex*, 24(1):17–36, 2014.

[29] Nikola T Markov and Henry Kennedy. The importance of being hierarchical. *Current opinion in neurobiology*, 23(2):187–94, apr 2013.

[30] Tiago Marques, Julia Nguyen, Gabriela Fioreze, and Leopoldo Petreanu. The functional organization of cortical feedback inputs to primary visual cortex. *Nature Neuroscience*, 21(5):757–764, 2018.

[31] Alberto Mazzoni, Stefano Panzeri, Nikos K Logothetis, and Nicolas Brunel. Encoding of naturalistic stimuli by local field potential spectra in networks of excitatory and inhibitory neurons. *PLoS computational biology*, 4(12):e1000239, dec 2008.

[32] David Meunier, Renaud Lambiotte, Alex Fornito, Karen D Ersche, and Edward T Bullmore. Hierarchical modularity in human brain functional networks. *Frontiers in neuroinformatics*, 3(October):1–12, 2009.

[33] Marc Mignard and Joseph G. Malpeli. Paths of information flow through visual cortex. *Science*, 251(4998):1249–1251, 1991.

[34] Rajesh P N Rao and Dana H. Ballard. Predictive coding in the visual cortex: A functional interpretation of some extra-classical receptive-field effects. *Nature Neuroscience*, 2(1):79–87, 1999.

[35] A. Shmuel. Retinotopic Axis Specificity and Selective Clustering of Feedback Projections from V2 to V1 in the Owl Monkey. *Journal of Neuroscience*, 25(8):2117–2131, 2005.

[36] Dan D. Stettler, Aniruddha Das, Jean Bennett, and Charles D. Gilbert. Lateral connectivity and contextual interactions in macaque primary visual cortex. *Neuron*, 36(4):739–750, 2002.

[37] M A Whittington, R D Traub, N Kopell, B Ermentrout, and E H Buhl. Inhibition-based rhythms: experimental and mathematical observations on network dynamics. *International journal of psychophysiology : official journal of the International Organization of Psychophysiology*, 38(3):315–36, dec 2000.

[38] W. Yang, Y. Carrasquillo, B. M. Hooks, J. M. Nerbonne, and A. Burkhalter. Distinct Balance of Excitation and Inhibition in an Interareal Feedforward and Feedback Circuit of Mouse Visual Cortex. *Journal of Neuroscience*, 33(44):17373–17384, 2013.